Purification and Characterization of Novel X and Y-family DNA Polymerases

A Senior Honor's Thesis

Presented in Partial Fulfillment of the Requirements for Graduation *with Research Distinction in Biochemistry* in the Undergraduate Colleges of the Ohio State University

by
Sean Alexander Newmister

The Ohio State University
June 2007

Project Advisor: Dr. Zucai Suo, Department of Biochemistry

Contents

A. Introduction

The story of evolution is one of heritable variation giving rise, over deep time, to the diversity of species that we observe today. At the time that Darwin put forth his theory nothing was known of the molecular phenomena which gave rise to that variation. However, with the structure of DNA solved and the subsequent advances in molecular biology, scientists have realized that such variation essential for evolution arises from a delicate balance of both the mutation and repair of an organism's genomic DNA. In order to understand how this balance is achieved, scientists have studied the pathways that bring about the faithful replication of genomic DNA as well those which are involved in correcting aberrant DNA modifications. The study of the underlying mechanisms of these pathways has led to the understanding of how deficiencies therein can give rise to genome instability, a condition which frequently results in tumor development and cancer formation.

My research is focused on a class of enzymes known as the DNA polymerases, which are directly involved in genome stability. DNA polymerases are instrumental to both the replication and maintenance of an organism's genomic DNA which is subject to numerous lesions such as mismatched bases, base loss, base modification, and double stranded breaks [4]. Many of these lesions if left unrepaired can stall replication complexes, which can be saved only by recruiting one of the recently discovered translesion polymerases [5]. DNA polymerases have been classified into six families A, B, C, D, X, and Y based on their phylogenetic relationships and they have been shown to participate in a diverse array of pathways in DNA metabolism [5].

I report here the purification of several DNA polymerases of both the X and Y-family. Due to the highly collaborative nature of modern research, much of the work that I have done has been part of a broader collaboration both within our lab and with laboratories in other departments or institutions. Throughout this thesis I report results both from my own research experience and from the experience of others. I have tried to be consistent throughout in specifying my unique contribution to the research and in all cases contributions made by others are acknowledged.

B. Nucleotide Binding in Human DNA Polymerase λ

Our interest in DNA polymerase λ began with the human genome project, which has revealed the existence of at least fifteen different DNA polymerases in humans. Prior to this discovery, it was commonly held that relatively few enzymes were required for the maintenance and replication of an organism's genome. Scientists have now undertaken the task of elucidating the biological role of these newly discovered DNA polymerases. Pol λ is one such enzyme, and while it shares 54% sequence homology with the well-characterized DNA polymerase β (Fig.1) [6, 7] recently acquired genetic and biochemical evidence suggests that the biological role of Pol λ is more complex. Due to its ability to carry out gap-filling DNA synthesis, Pol β has been established as the acting polymerase in the major pathway to repair single base lesions [8, 9] known as the base excision repair pathway (BER). Because of their sequence homology and shared catalytic activities, it has been hypothesized that Pol λ also functions in BER *in vivo* [10, 11]. Other evidence suggests that Pol λ may also participate in V(D)J recombination and non-homologous end joining (NHEJ) pathways *in vivo* [12, 13]. Pol λ, unlike any other characterized DNA polymerase, is unique in its ability to bind all nucleotides, correct or incorrect, with high binding affinity [11]. DNA polymerases typically bind two ligands: DNA and an incoming nucleotide. Most DNA polymerases, including Pol β, discriminate against the incorporation of incorrect nucleotides by binding them weakly [14]. Data gathered in our lab, however, shows that the ground-state binding affinity (K_d) of all nucleotides in Pol λ is both tight and nonselective [11]. This phenomenon is of particular interest to us because many chemotherapeutic agents gain their efficacy by mimicking endogenous

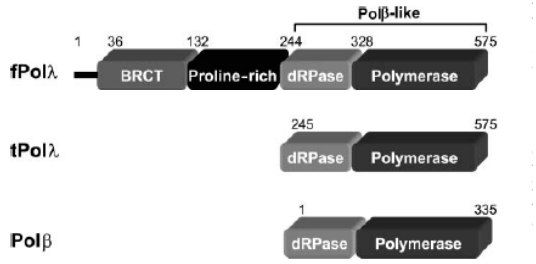

Fig. 1. Domain structure of full-length hPol λ, truncated (β-like) hPol λ, and hPol β

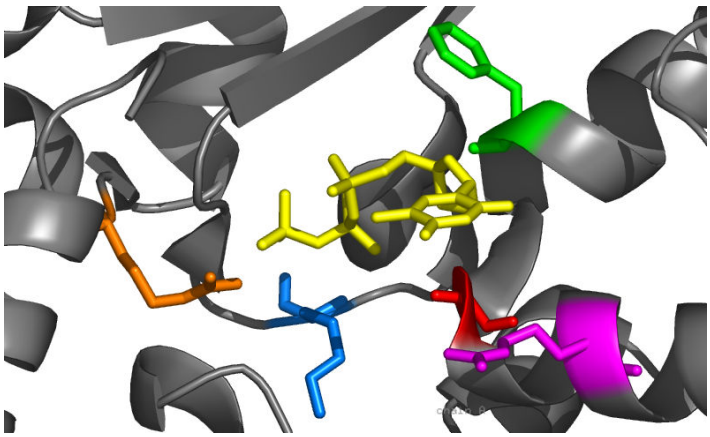

Fig. 2. Close view of tPolλ•DNA•ddTTP active site [2]. Residues R386, K422, F506, A510, and R514 are shown as sticks surrounding the incoming nucleotide (ddTTP).

nucleotides, but of the 30 nucleoside analogues approved by the FDA, none have been studied in the context of Pol λ because the enzyme was discovered after their approval. The putative role of Pol λ in DNA repair lends particular significance to Pol λ's interaction with chemotherapeutic agents. The aim of this project was to establish the structural basis for the interactions between Pol λ and incoming nucleotides. By examining the crystal structure for tPol λ in complex with gapped DNA and an incoming nucleotide (Fig. 2), a series of residues proposed to interact with the incoming nucleotide were identified. After carrying out site-directed mutagenesis on six residues: R386, K422, F506, A510, R514, and R517, we have identified three residues, R386, A510, and R514 that play a significant role in high binding affinity of incoming nucleotides both correct and incorrect. Based on the crystal structure of the tPol λ ternary complex, we believe that residue R386 interacts with the γ-phosphate of the incoming nucleotide by the formation of a salt bridge. Residue A510 interacts with the base of the incoming nucleotide by *van der Waal's* interactions. Residue R514 is positioned at the interface between the DNA template and the incoming nucleotide. As a result, it acts to both stabilize the incoming nucleotide and the DNA template.

Experimental Procedures

Generation of hPolλ mutants. All mutants used in this study were generated by Dr. Suo's Biochemistry 521 course (Winter 2005) using site-directed mutagenesis.

Purification of hPolλ mutants. The N and C-terminal His_6-tagged hPol λ mutant plasmids (pET 28b) were transformed into BL21 (DE3) RIL chemical competent cells by heat shock (42° C for 45 seconds). An overnight culture of *E. coli* expression strain BL21(DE3) RIL carrying the mutant plasmid was used to inoculate Luria-Bertani medium containing 40 μg/mL kanamycin and 25 μg/mL chloramphenicol, and the cells were grown at 37° C until OD_{600} = 0.6. The cultures were induced with 0.15 mM IPTG and incubated at 19° C for 9 h (OD_{600} ~1.7). Induced cells were harvested (4000 rpm,15 min) and resuspended in Buffer A (10 mM $KHPO_4$, pH 7.0, 500 mM NaCl, 10 mM $MgCl_2$, 10% glycerol, 0.1% beta-mercaptoethanol, 1 mM imidazole). EDTA-free protease inhibitor cocktail (Roche, 1 tablet) and PMSF (1 mM) were added just before cell lysis. Cells were lysed by passing through a French Press cell at 15,000 psi three times, and the lysate was clarified by ultracentrifugation (40,000 rpm, 40 min). The supernatant was incubated with 8 ml IMAC Fastflow6 resin (Ni^{2+} charged, GE Healthcare) and rocked slowly for 3 hours in the presence of 10 mM imidazole. The supernatant was then

removed by centrifugation in a swing bucket centrifuge (2500 rpm, 2.5 min) and the resin was packed into the HR-10/10 FPLC column. The hPol λ bound to the resin was purified through a linear gradient of 35–500 mM imidazole in Buffer B (10 mM $KHPO_4$, pH 7.0, 350 mM NaCl, 5—500 mM Imidazole, 10% Glycerol, 0.05% β-mercaptoethanol). Fractions containing hPol λ were dialyzed for 3 hours against dialysis Buffer C (25 mM HEPES, pH 7.0 at 4° C, 100 mM NaCl, 1 mM EDTA, 10% Glycerol, 0.1% β-mercaptoethanol). The dialyzed protein solution was applied to a Heparin Sepharose Fast Flow column (GE Healthcare) and eluted using 100–1000 mM NaCl in buffer C. Fractions containing hPol λ were pooled and dialyzed against buffer C. The dialyzed hPol λ was passed through two 5 mL HiTrap Q anion exchange columns (GE Healthcare). The loading elute was applied to two 5 mL HiTrap SP cation exchange columns (GE Healthcare) and eluted using a gradient of 100—1000 mM NaCl in buffer C. The fractions containing hPol λ were dialyzed against buffer D (25 mM HEPES, pH 7.0 at 4° C, 150 mM NaCl, 1 mM EDTA, 1 mM DTT, 50% Glycerol) and stored at -80° C. The concentration of the purified hPol λ mutants were measured spectrophotometrically at 280 nm using the calculated extinction coefficient 61,615 $M^{-1}cm^{-1}$.

Determination of the k_p and K_d of an Incoming Nucleotide. The 21-19/41-mer DNA substrate (Fig. 3A) was purified by denaturing polyacrylamide gel electrophoresis and prepared as described [11]. A solution containing hPolλ (120 nM) and 5'-[^{32}P] DNA (30 nM) preincubated in buffer L (50 mM Tris-HCl, pH 8.4 at 37° C, 5 mM $MgCl_2$, 100 mM NaCl, 0.1 mM EDTA, 5 mM DTT, 10% glycerol, and 0.1 mg/mL BSA) was mixed with increasing concentrations of a single nucleotide. Reactions were terminated by the addition of 0.37 M EDTA. Products were separated from remaining substrate via sequencing gel electrophoresis (17% acrylamide, 8 M urea) (Fig. 3B.) and quantitated using a

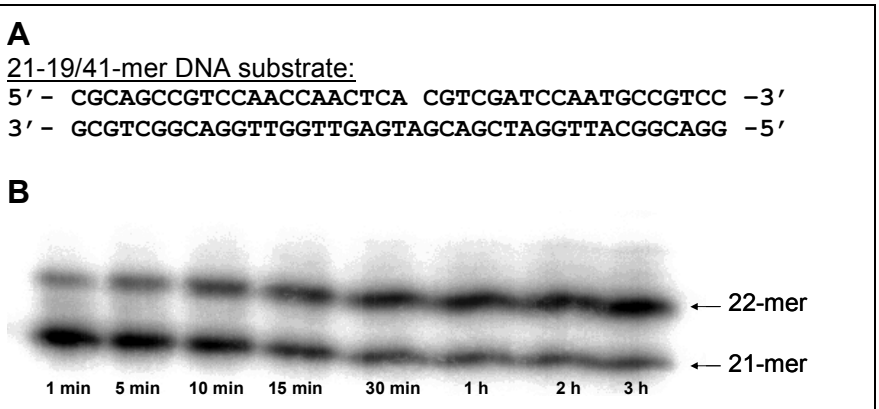

Fig. 3. Pre-steady-state kinetic assay. A preincubated solution of hPolλ mutant and 21-19/41-mer substrate were mixed with a single dNTP for various reaction times before quenching with EDTA. A**,** 21-19/41-mer substrate. B, products are resolved by gel electrophoresis on a 17% Acrylamide, 8 M urea, 1 X TBE gel.

PhosphorImager 445 SI (Amersham Biosciences). The time course of product formation was fit to Equation 1 for each concentration of dNTP to yield an observed rate constant (k_{obs}) and a reaction amplitude (A). The extracted k_{obs} values were then plotted as a function of the concentration of dNTP and fit to Equation 2 to give k_p and K_d.

(Eq. 1)

$$[\text{product}] = A[1-\exp(-k_{obs}t)]$$

(Eq. 2)

$$k_{obs} = k_p[\text{dNTP}]/\{[\text{dNTP}] + K_d\}$$

Data were fit by nonlinear regression using the program KaleidaGraph (Synergy Software).

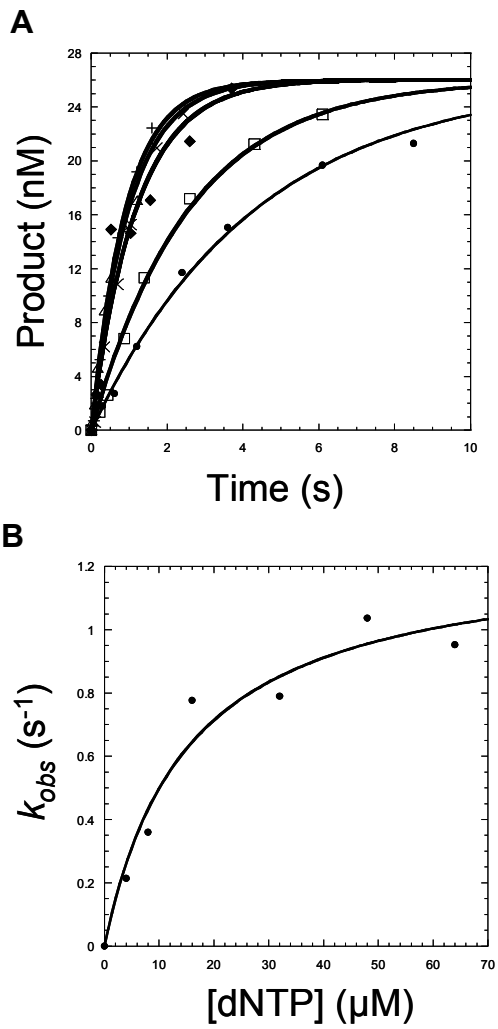

Fig. 4. Data Fitting. A, Solid lines are best fits to single-exponential equation. B, Solid line is best fit to hyperbolic equation.

Summary of Results

Based on the K_d values recorded in Table 1 it was concluded that, of the six residues mutated, residues R386, A510, and R514 play the major role in nucleotide binding. By examining the crystal structure of the tPol λ ternary complex, one can readily observe the strong salt bridge formation between the negatively charged γ-phosphate on the dNTP and the positively charged guanidinium group on R386. Although this residue is conserved in Pol β, the measured distance of the salt bridge is 6.14 Å [15] which accounts for a weaker stabilization when compared to the 4.39 Å distance in the tPol λ ternary structure. The mutation of residue A510 to glutamate can also be understood by examining the crystal structure, which reveals that the 510 position is sufficiently close to the dNTP that an introduced carboxylate would repel the negatively charged α-phosphate of the dNTP. This phenomenon has been observed in Pol β, which has an aspartate at the corresponding position in the wild-type enzyme. A similar difference between tPol λ and Pol β can also be

Correct dTTP incorporation:		
Enzyme	K_d (μM)	K_d ratio[a]
R386A	15 ± 5	5.8
K422A	7 ± 1	2.5
F506A	8 ± 4	3.0
A510E	7 ± 2	2.7
R514A	12 ± 4	4.6
Wild-type	2.6 ± 0.4	1
Incorrect dTTP incorporation:		
Enzyme	K_d (μM)	K_d ratio[a]
R386A	35 ± 4	11
K422A	5.5 ± 0.6	1.7
F506A	19 ± 6	5.9
A510E	31 ± 20	9.7
R514A	63 ± 24	20
Wild-type	3.2 ± 0.5	1

Table 1. Measured K_d of nucleotide incorporation for all mutants.

[a]Calculated as $K_{d\ mutant}$/ $K_{d\ wild\text{-}type}$.

observed in the instance of Pol λ R514, which demonstrates multiple close interactions > 6.5 Å with the DNA template and the dNTP. In the corresponding residue, K280, in Pol β no interactions with the dNTP can be observed in the crystal structure [15].

C. Structure-Function Studies in *Sulfolobus solfataricus* DNA polymerase IV (Dpo4)

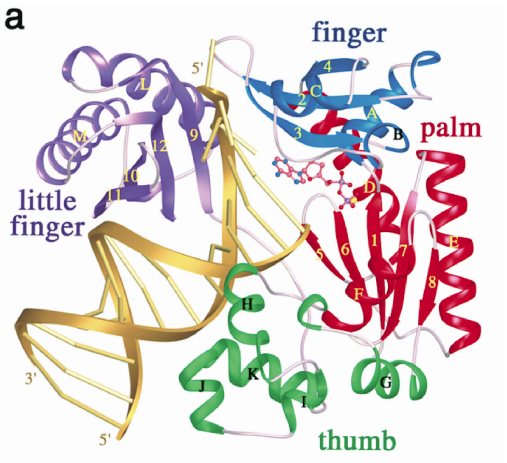

Fig. 5. Structure of the Dpo4•13-mer/ 18-mer•dADP complex. [3]

Genomic DNA is continually subjected to a myriad of endogenous and exogenous DNA damaging agents such as UV light, reactive oxygen species, and ionizing radiation [16]. Cellular mechanisms that repair DNA lesions have evolved, but many lesions elude DNA repair pathways and persist, thereby impeding DNA replication. In order to survive, cells must have the means to carry out DNA replication even in the presence of DNA lesions. Canonical DNA replication complexes, however, are incapable of synthesis through DNA lesions due to their restrictive active sites. Stalled replication complexes can be saved by the recruitment of a novel class of enzymes known as the Y-family DNA polymerases. The recently discovered Y-family DNA polymerases can be found in all domains of life and have been shown to be capable of translesion synthesis [17]. The ability to carry out lesion bypass is granted by a relatively flexible active site that can accommodate aberrant base pairing geometries. Consequently, the Y-family polymerases are characterized by a low-processivity and demonstrate low-fidelity. Because of its ease of purification [18] and ability to carry out tranlesion synthesis, *Sulfolobus solfataricus* DNA polymerase IV (Dpo4), has served as a model Y-family enzyme in a variety of studies in our lab [18-21], and continues to provide more avenues for fruitful research. Four studies with Dpo4 are described in this report. In the first project the nature of a region of Dpo4 known as the linker region was interrogated in the context of DNA binding. The next two studies were more biophysical in nature, with the first being an attempt to crystallize Dpo4 in the presence of a blunt-ended DNA substrate and an incoming nucleotide, and the second being a fluorescence up-conversion assay to probe the dynamics of the enzyme active site. Lastly, Dpo4 has been used in a protein engineering effort with the ultimate goal of engineering a fused construct of Dpo4 and an ATP-dependent translocase that will effectively motor the polymerase along a single-stranded DNA substrate.

1. DNA Binding Studies with Dpo4 All Glycine Linker and Dpo4-Dbh Linker Swap:

By studying a model Y-family polymerase, *Sulfolobus solfataricus* DNA Polymerase IV, we seek to investigate the role of a unique domain known as the little finger, which is thought to grant this enzyme its essential lesion bypass characteristics [3, 17, 22]. The little finger domain in Dpo4 is tethered to the core of the polymerase by a filament called the linker region. Preliminary work has shown that the size of the linker region significantly affects the enzyme's ability to form stable binding complexes with primed DNA substrates. By generating a series of mutant Dpo4 enzymes, each with a linker region of different size, and measuring the ground-state DNA binding affinity (K_d) using gel electrophoretic mobility shift assays and fluorescence titration assays (Jun Zhang and Suo, unpublished data) (Table 2) we hypothesize that the linker size has been optimized by nature for the best possible DNA binding. However, this data leaves many unanswered questions regarding the linker region's role in DNA binding. The most notable ambiguity is the impact that amino acid composition may have regarding the linker region's interactions with DNA. Therefore, we began a series of studies in which the size of the linker region is left unmodified, but the amino acid composition will be varied using site directed mutagenesis. The first mutation assayed was an "all-glycine linker" mutant in which all of the original 14 amino acid residues in the linker region were mutated to glycine. Glycine was chosen for this purpose because it has no side chains that may interact with the DNA and it also confers the most flexibility to the peptide backbone [23]. The second mutation assayed was the Dpo4-Dbh linker swap mutant. This mutation was inspired by the work of Boudsocq et. al. which demonstrated that by swapping the linker region and little finger domains of Dpo4 and Dbh the enzymatic properties could be also be "swapped." By assaying these mutants we will better understand the role of this novel domain in lesion bypass catalyzed by the Y-family polymerases.

Enzyme	Linker Sequence	K_D
WT	RDEYNEPIRTRVRK	10 nM
1 Gly Addition	RDEYNEPIGRTRVRK	118 nM
4 Gly Addition	RDEYNEPIGGGGRTRVRK	279 nM
6 Gly Addition	RDEYNEPIGGGGGGRTRVRK	674 nM
1 Deletion	RDEYNEP-RTRVRK	159 nM
4 Deletion	RDEY----RTRVRK	304 nM
6 Deletion	RD------RTRVRK	1688 nM

Table 2. DNA binding data for Dpo4 linker mutants.

Experimental Procedures

Generation of the Dpo4 All-glycine linker Mutant and Dpo4-Dbh linker swap Mutant. Synthetic oligonucleotide primers (Table 3) were used to generate the Dpo4 linker mutants via a site-directed mutagenesis kit using *Pfu Turbo* (Stratagene). The Dpo4-Dbh linker swap mutant was generated over three rounds, with the plasmid resulting from each round serving as the template for the subsequent rounds of mutagenesis. The 14 amino acid sequence of the Dpo4 linker (RDEYNEPIRTRVRK) was mutated to that of Dbh (RNKYSEPVENKSKI). The Dpo4 all-glycine linker mutant was generated using one round of mutagenesis. PCR was carried out for 18 cycles (denaturation, 95° C for 30 sec; annealing, 48° C for 1 min; extension, 68° C for 14 min) and after DpnI digestion the amplified products were transformed into the XL-10 Gold *E.coli* strain (Stratagene). Mutant plasmids were purified from transformed cells using the Wizard *Plus* SV Miniprep kit (Promega) and sequences were confirmed by OSU Plant Microbe Genomics Facility.

Table 3. DNA primers for Site-Directed-Mutagenesis

Dbh L-1	Forward 5'-GAGTATAACGAGCCTGTAGAAAATAGATCAAAAATCAGTATTGGGAGAATTG -3' Reverse 5'-CAATTCTCCCAATACTGATTTTTGATCTATTTTCTACAGGCTCGTTATACTC -3'
Dbh L-2	Forward 5'-GCTAAGGCTAAATATCTGATCTCTCTAGCCAGAGACGAGTATAAC -3' Reverse 5'-GTTATACTCGTCTCTGGCTAGAGAGATCAGATATTTAGCCTTAGC -3'
Dbh L-3	Forward 5'-CTGATCTCTCTAGCCAGAAACAAGTATAGCGAGCCTGTAGAAAATAG -3' Reverse 5'-CTATTTTCTACAGGCTCGCTATACTTGTTTCTGGCTAGAGAGATCAG -3'
All Gly	Forward 5′-GCTAGAGACGGGGGTGGCGGGGGTGGAGGAGGTGGAGGAGGAGGGAGTATTGGG –3′ Reverse 5′-CCCAATACTCCCTCCTCCTCCACCTCCTCCACCCCCGCCACCCCCGTCTCTAGC -3′

Purification of the Dpo4 All-Glycine linker and Dpo4-Dbh Linker swap mutants. The C-terminal His_6-tagged Dpo4 All-gly linker and Dpo4-Dbh Linker swap plasmids (pET 22b+) were transformed into BL21(DE3) RIL chemical competent cells by heat shock (42° C for 45 seconds). An overnight culture of *E. coli* expression strain BL21(DE3) RIL carrying the Dpo4 plasmid was used to inoculate Luria-Bertani medium containing 100 µg/mL ampicilan, and the cells were grown at 37° C until OD_{600} = 0.6. The cultures were induced with 0.15 mM IPTG and incubated at 30° C for 5.5 h (OD_{600} ~1.7). Induced cells were harvested (4000 rpm,15 min) and resuspended in Buffer A (10 mM $KHPO_4$, pH 7.0, 50 mM NaCl, 10 mM $MgCl_2$, 10% glycerol, 0.1% beta-mercaptoethanol, 1 mM imidazole). PMSF (1 mM) was added just before the cells were lysed by passing through a French Press cell at 15,000 psi three times, and the

lysate was clarified by ultracentrifugation (40,000 rpm, 40 min). Cleared lysate was subjected to heat denaturation at 78° C for 12 min to precipitate thermolabile *E. coli* proteins which were then removed by ultracentrifugation (40,000 rpm, 40 min). The supernatant was incubated with 8 ml IMAC Fastflow6 resin (Ni^{2+} charged, GE Healthcare) and rocked slowly for 3 hours in the presence of 10 mM imidazole. The supernatant was then removed by centrifugation in a swing bucket centrifuge (2500 rpm, 2.5 min) and the resin was packed into a HR-10/10 FPLC column (GE Healthcare). The Dpo4 bound to the resin was purified through a linear gradient of 35–500 mM imidazole in Buffer B (10 mM $KHPO_4$, pH 7.0, 350 mM NaCl, 5–500 mM imidazole, 10% Glycerol, 0.05% β-mercaptoethanol). Fractions containing Dpo4 were dialyzed for 3 hours against dialysis Buffer C (50 mM Tris-HCl, pH 7.5 at 25° C, 50 mM NaCl, 1 mM EDTA, 10% Glycerol, 0.1% β-mercaptoethanol). The dialyzed protein solution was passed through two 5 mL HiTrap Q anion exchange columns (GE Healthcare). The loading elute was applied to two 5 mL HiTrap SP cation exchange columns (GE Healthcare) and eluted using a gradient of 100—1000 mM NaCl in buffer C. The fractions containing Dpo4 were dialyzed against buffer D (25 mM HEPES, pH 7.0 at 4° C, 150 mM NaCl, 1 mM EDTA, 1 mM DTT, 50% Glycerol) and stored at -80° C. The concentrations of the purified Dpo4 mutants were measured spectrophotometrically at 280 nm using the calculated extinction coefficient 24,580 $M^{-1}cm^{-1}$.

Fluorescence Titration Assay. The binding affinity of the Dpo4 mutant enzymes for a DNA duplex was carried out using a fluorescence titration assay. Varying concentrations of Dpo4 (6.3-300 nM) were titrated into a quartz cuvette containing a 23/34-mer 2-Aminopurine (2-AP)-embedded substrate (Fig. 6). The excitation wavelength for the Dpo4•23/34-mer duplex was 310 nm, and the emission was recorded from 360–400 nm. All quantitation was carried out using the emission at 370 nm. Emission intensity was corrected to measure the contribution of the Dpo4•DNA complex only by subtracting the emission of buffer

A

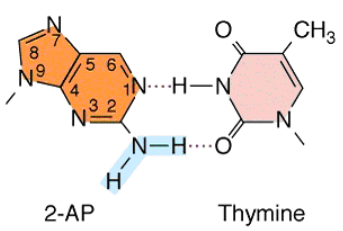

B

5′-CGCAGCCGTCCAACCAACTCAG-3′
3′-GCGTCGGCAGGTTGGTTGAGTC**X**CAGCTAGGTTA-5′

Fig. 6. A, 2-AP structure. B, 23/34-mer DNA substrate. Bold '**X**' indicates 2-AP.

alone and DNA alone contribution. The resulting fluorescence was fit to a quadratic binding equation (Eq. 4), which was derived from Equation 3 by substituting the fluorescence signal for [ES].

(Eq. 3)

$$[ES] = \frac{(K_D + [S_T] + [E_T]) - \sqrt{(K_D + [S_T] + [E_T])^2 - 4[S_T][E_T]}}{2}$$

(Eq. 4)

$$F = F_I + (F_T - F_I)\frac{(K_D + [S_T] + [E_T]) - \sqrt{(K_D + [S_T] + [E_T])^2 - 4[S_T][E_T]}}{2}$$

Summary of Results

Using a fluorescence titration assay a K_d of 6.7 nM was obtained for the Dpo4 Dbh linker swap mutant and the exact quantitation of the K_d for the Dpo4 all-glycine linker mutant has been delayed by technical complications with the fluorometer, however our preliminary results indicate that the DNA binding affinity of the all-glycine mutant is comparable to that of wild-type. The K_d value of the Dpo4 Dbh linker swap mutant differs only slightly from the wild-type K_d of 4.5 nM. Based on these results we can conclude that linker size, as opposed to sequence, is the key factor in determining the strength of DNA binding by the Dpo4 enzyme. These results also indicate that the unique enzymatic properties granted by the little finger domain [22] are not dependent on the composition of the linker region despite the fact that only 29% homology is shared between Dpo4 and Dbh in the 14 amino acid linker region.

2. Crystallization of Dpo4•13-mer/18-mer•dATP and Dpo4•13-mer/13-mer•dATP Ternary Complexes:

Recent studies of the reverse transcriptase enzyme encoded by the human immunodeficiency virus 1 reveal a unique ability to make single nucleotide additions to blunt-ended DNA substrates [24, 25]. This activity offers a plausible mechanism by which the HIV-1 virus is able to mutate with such high efficiency and thus elude contemporary medicine's best efforts to eradicate the virus from our population [25, 26]. The model enzyme Dpo4 was used to interrogate the mechanism such blunt-end additions to DNA. Previous kinetic experiments have shown this model enzyme to be capable of similar blunt-end addition as described for HIV1-RT. In order to determine the structure by x-ray crystallographic methods, we sought to crystallize a ternary complex of the enzyme, blunt-ended DNA substrate, and an incoming deoxynucleotide. A complete structure, through analysis of the geometry of the ternary complex, would provide strong evidence for the proposed mechanism of single nucleotide addition at free DNA blunt ends. It was our expectation that the incoming nucleoside triphosphate would form an interstrand base stacking interaction with the 5' end of the template DNA. This base stacking could provide an adequate amount of energy to temporarily immobilize the nucleoside triphosphate in an orientation that is favorable for the chemistry of phosphodiester bond formation. In working toward this goal a structure for the ternary complex with a blunt-ended DNA substrate was not obtained in our lab, but instead by our collaborator, Dr. Hong Ling. While we were unsuccessful in generating diffracting crystals with the blunt-ended substrate, we were able to obtain crystals and solve the structure of the control setup which contained a 13/18-mer DNA substrate.

Table 4. DNA substrates.

Dpo4•13-mer/18-mer•dATP
5'-GGCTACAGGACTC-3' 13mer
3'-CCGATGTCCTGAGTACTT-5' 18mer

Dpo4•13-mer/13-mer•dATP
5'-GGCTACAGGACTC-3' 13mer
3'-CCGATGTCCTGAG-5' 13mer

Experimental Procedures

Purification of Native Dpo4. The native Dpo4 plasmid (p1914) was transformed into BL21(DE3) electrocompetent cells by electroporation. An overnight culture of E. coli expression strain BL21(DE3) carrying the native Dpo4 plasmid was used to inoculate Luria-Bertani medium containing 100 µg/mL ampicilan, and the cells were grown at 37° C until OD_{600} = 0.6. The cultures were induced with 0.2 mM IPTG and incubated at 34° C for 4.5 h (OD_{600}

~1.7). Induced cells were harvested (4000 rpm,15 min) and resuspended in Buffer A (10 mM $KHPO_4$, pH 7.0, 50 mM NaCl, 10 mM $MgCl_2$, 10% glycerol, 0.1% beta-mercaptoethanol). PMSF (1 mM) was added just before the cells were lysed by passing through a French Press cell at 15,000 psi three times, and the lysate was clarified by ultracentrifugation (40,000 rpm, 40 min). Cleared lysate was subjected to heat denaturation at 80° C for 12 min to precipitate thermolabile E. coli proteins which were then removed by ultracentrifugation (40,000 rpm, 40 min). The supernate was applied to a Heparin Sepharose column (GE Healthcare) and eluted by a linear gradient (50–1000 mM NaCl) in buffer B (20 mM HEPES, pH 7.0 at 4°C, 100 mM NaCl, 1 mM EDTA, 10% Glycerol, 0.1% β-mercaptoethanol). Fractions containing Dpo4 were dialyzed against buffer B (50 mM NaCl) for 3 h at 4° C. The dialyzed protein solution was passed through two 5 mL HiTrap Q anion exchange columns (GE Healthcare). The loading elute was applied to two 5 mL HiTrap SP cation exchange columns (GE Healthcare) and eluted using a gradient of 100—1000 mM NaCl in buffer B. The fractions containing Dpo4 were dialyzed against buffer C (20 mM HEPES, pH 7.0 at 4° C, 100 mM NaCl, 1mM DTT, 5mM $MgCl_2$, 2.5% glycerol) for 3 h at 4° C, and the dialyzed protein solution was concentrated to 16 mg/mL (381 μM) using a Centriprep YM-10 apparatus. The concentration of the purified Dpo4 was measured spectrophotometrically at 280 nm using the calculated extinction coefficient 24,580 $M^{-1}cm^{-1}$.

Synthetic Oligonucleotides. DNA substrates were purified using polyacrylamide gel electrophoresis and desalted using reverse-phase chromatorgraphy (Sep-pack C_{18}). The concentration of the DNA primers was measured spectrophotometrically using the extinction coefficients provided by the manufacturer (Integrated DNA Technologies; 13-mer: 123,300 M^{-1} cm^{-1}, 18-mer 166,500 $M^{-1}cm^{-1}$). The 13-mer substrate was dideoxy-terminated at the 3' end in order to prevent reaction with the incoming dATP, which would result in a heterogeneous mixture of DNA substrate in the complex.

Crystallization Conditions. The optimal conditions for crystallization of Dpo4 were established in 2001 [3], and the setup for both the Dpo4•13-mer/18-mer•dATP and the Dpo4•13-mer/13-mer•dATP complexes were based on only slight variation from the optimal conditions for the *well solution* (16% PEG 3350, 0.1 M HEPES, pH 7.0, 100 mM $Ca(OAc)_2$,

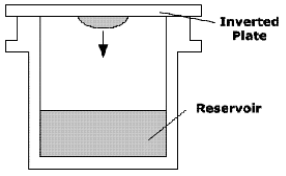

Fig. 7. Hanging-drop vapor diffusion apparatus

2.5% glycerol) and *drop solution* (60 mM NaCl, 5 mM $MgCl_2$, 1 mM DTT, 1 mM dATP, 8 mg/mL Dpo4, 228.6 µM DNA, 20 mM HEPES, pH 7.0, 2.5% glycerol). Numerous hanging drop vapor diffusion apparatus were set up using the stated conditions, and others were set up with slight variations in pH (6.75–7.25) and PEG (10–16%). In all cases the ratio of DNA:Dpo4 was held at a constant 1.12:1 ratio [3]. After set up the trays were left undisturbed at 25° C for 48 h before being examined for crystal growth.

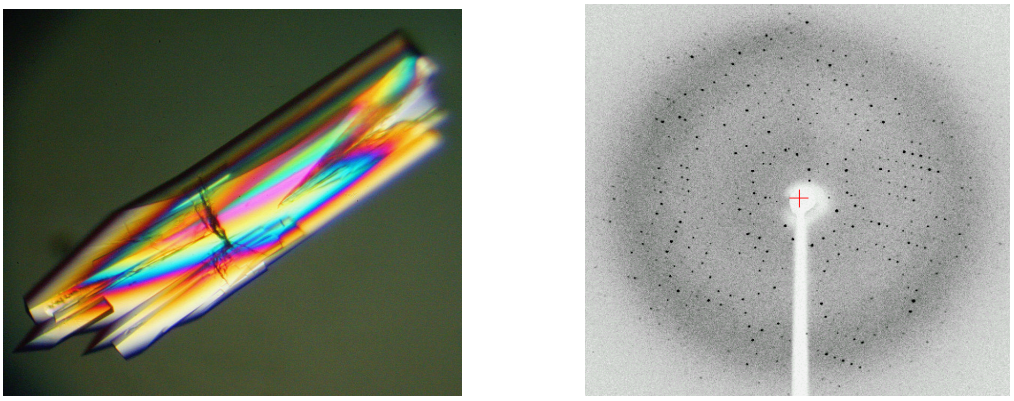

Fig. 8. Crystal (left) and X-ray diffraction pattern (right) of Dpo4•13-mer/18-mer•dATP complex. Resolution observed at OSU X-ray diffraction facility: 2.5 Å.

Summary of Results

While the ultimate goal of this project was in fact to obtain diffracting crystals of the Dpo4•13-mer/13-mer•dATP complex in order to understand the mechanism of blunt-end addition by a DNA polymerase, the task was ultimately deferred to our collaborator Dr. Hong Ling. We were able to obtain diffracting crystals (Fig. 8) of the Dpo4•13-mer/17-mer•dATP complex and the structure was solved using the molecular replacement technique by Jason Fowler, a gradient student in our lab. The structure for this complex has already been solved [3], but the our efforts were regardless a worthwhile exercise in the crystallization of polymerases, and the results of the blunt-end addition study were published in 2007 [19], using the structure provided by Dr. Hong Ling.

3. Purification of Dpo4 Y12W and Y312W Mutants:

Fluorescence spectroscopy of the aromatic amino acid residues offers a very sensitive probe in detecting protein molecular conformational changes. Sometimes rather subtle changes in the conformation of a protein give rise to fairly large changes in the fluorescence characteristics, whereas other physical methods fail to show any change [1]. Since the protein conformational changes take place very quickly, the events have to be resolved on a pico or femto second scale. The femtosecond resolved fluorescence of a protein containing a single tryptophan residue using LASER are used to study the dynamics of protein function. The fluorescence intensity is affected by specific interactions and by solvent and environmental factors (hydration).

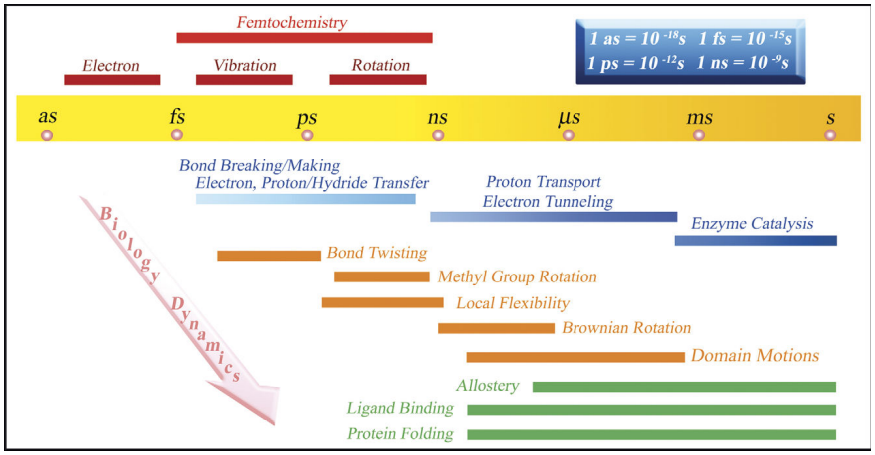

Fig.9. Timescale of fundamental motions, chemistry, and dynamics [1].

Dpo4, a Y-family DNA polymerase from *Sulfolobus solfataricus* is can bypass various DNA lesions. It has 16 tyrosine residues whereas no tryptophan residues. In order to probe the dynamics of Dpo4 function, Dpo4 was mutated to contain a single tryptophan residue at its active site (Y12W) and purified to near homogeneity. The Y12 residue is located in the finger domain. As a control another Dpo4 mutant with tryptophan on the surface (Y312W) was made and purified.

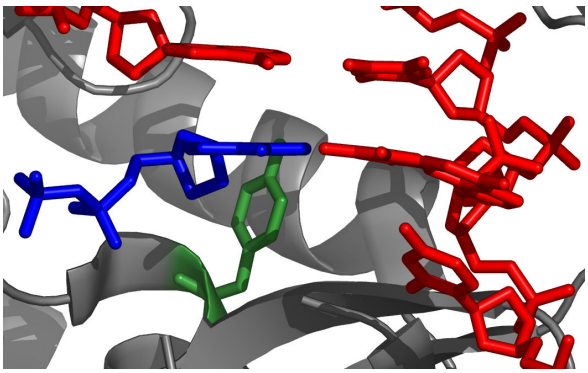

Fig. 10. Close view of Dpo4 active site. Y12 is shown in close proximity to the incoming dATP (left) [3].

Experimental Procedures

Generation of Dpo4 Y12W and Y312W. The single substitution mutants were generated using site-directed mutagenesis by the students in Dr. Suo's Biochemistry 521 course.

Purification of Dpo4 Y12W and Y312W. The C-terminal His_6-tagged Dpo4 Y12W and Y312W plasmids (pET 22b+) were transformed into BL21 (DE3) chemical competent cells by heat shock (42° C for 45 seconds). An overnight culture of *E. coli* expression strain BL21(DE3) carrying the Dpo4 plasmid was used to inoculate Luria-Bertani medium containing 100 µg/mL ampicilan, and the cells were grown at 37° C until OD_{600} = 0.6. The cultures were induced with 0.15 mM IPTG and incubated at 30° C for 5.5 h (OD_{600} ~1.7). Induced cells were harvested (4000 rpm,15 min) and resuspended in Buffer A (10 mM $KHPO_4$, pH 7.0, 50 mM NaCl, 10 mM $MgCl_2$, 10% glycerol, 0.1% beta-mercaptoethanol, 1 mM imidazole). PMSF (1 mM) was added just before the cells were lysed by passing through a French Press cell at 15,000 psi three times, and the lysate was clarified by ultracentrifugation (40,000 rpm, 40 min). Cleared lysate was subjected to heat denaturation at 78° C for 12 min to precipitate thermolabile *E. coli* proteins which were then removed by ultracentrifugation (40,000 rpm, 40 min). The supernatant was incubated with 10 ml IMAC Fastflow6 resin (Ni^{2+} charged, GE Healthcare) and rocked slowly for 3 hours in the presence of 10 mM imidazole. The supernatant was then removed by centrifugation in a swing bucket centrifuge (2500 rpm, 2.5 min) and the resin was packed into a HR-10/10 FPLC column (GE Healthcare). The Dpo4 bound to the resin was purified through a linear gradient of 35–500 mM imidazole in Buffer B (10 mM $KHPO_4$, pH 7.0, 350 mM NaCl, 5–500 mM Imidazole, 10% Glycerol, 0.05% β-mercaptoethanol). Fractions containing Dpo4 were dialyzed for 3 hours against dialysis Buffer C (50 mM Tris-HCl, pH 7.5 at 25° C, 50 mM NaCl, 1 mM EDTA, 10% Glycerol, 0.1% β-mercaptoethanol). The dialyzed protein solution was passed through two 5 mL HiTrap Q anion exchange columns (GE Healthcare). The loading elute was applied to three 5 mL HiTrap SP cation exchange columns (GE Healthcare) and eluted using a gradient of 100—1000 mM NaCl in buffer C. The fractions containing Dpo4 were dialyzed against buffer D (50 mM Tris-HCl, pH 7.5 at 25° C, 300 mM NaCl, 1 mM EDTA, 10% Glycerol) for 3 h at 4° C. TCEP (1 mM) was added to the protein solution which was concentrated using a Centriprep YM-10 apparatus. The protein solution was examined every 5 min during concentration to ensure that no precipitation had occurred. The concentrations of the purified Dpo4 mutants were measured

spectrophotometrically at 280 nm using the calculated extinction coefficient 26,360 $M^{-1}cm^{-1}$ and stored at -80° C. The final concentration for Dpo4 Y12W was 343 μM and 350 μM for Dpo4 Y312W. High protein concentration was needed to provide sufficient signal for fluorescence up-conversion assays. Dpo4 could not be concentrated beyond 350 μM without precipitation.

Summary of Results

Upon purification and concentration, the Dpo4 Y12W and Y312W mutants were given to our collaborator Dr. Dongping Zhong in the Department of Physics at OSU. All results obtained thus far have proved inconclusive. The Y12W and Y312W mutants demonstrate a fluorescence change that is comparable in magnitude. This could be due to two phenomena: (1) that the Y312W mutant is not serving as a control in the manner we anticipated because the nature of solvation changes during the catalytic cycle, or (2) high NaCl concentrations in buffer D have resulted in a substantial reduction in enzyme activity, which reduces the anticipated fluorescence of the Y12W mutant.

4. Generation of *E.coli* UvrD•Dpo4 Fusion Construct

In this project it was our aim to generate a fusion protein which tethered a DNA polymerase to an ATP-dependent translocase in an attempt to amplify the processivity of Dpo4, a non-processive enzyme. We planned to fuse a motor protein at the C-terminus of Dpo4 in order to provide it with the ATP-dependant energy required to translocate along template DNA. Translocases/helicases are one of the best studied classes of DNA translocating enzymes. In order to select candidate motor protein for Dpo4, the translocase/helicase proteins from archaea and bacteria were examined. The archaeal enzymes are not well characterized in terms of their kinetics, processivity, or oligomeric status. The bacterial translocases, however, have been well characterized, e.g. Rep helicase, RecBCD and Helicase II (UvrD) and PcrA. The *E. coli* Rep helicase and PcrA from gram negative bacteria have high rates of translocation but only moderate processivity [27]. *E. coli* helicase II (UvrD) has high processivity of DNA translocation and it is capable of translocating ssDNA in 3' to 5' direction in monomeric form [28]. Based on these facts the UvrD translocase/helicase was selected to fuse with Dpo4. It is encoded by the uvrD gene and functions in a number of DNA repair processes including (i) methyl directed mismatch repair and (ii) excision repair [28, 29]. It is DNA dependant helicase and belongs to superfamily I of DNA helicases. At low concentrations it preferentially unwinds duplex DNA with 3' single-stranded tails but at higher concentrations it can initiate DNA unwinding at blunt ends and at nicks [28]. Hence it is believed to unwind duplex DNA during these repair processes, however its mechanism of unwinding is not fully known.

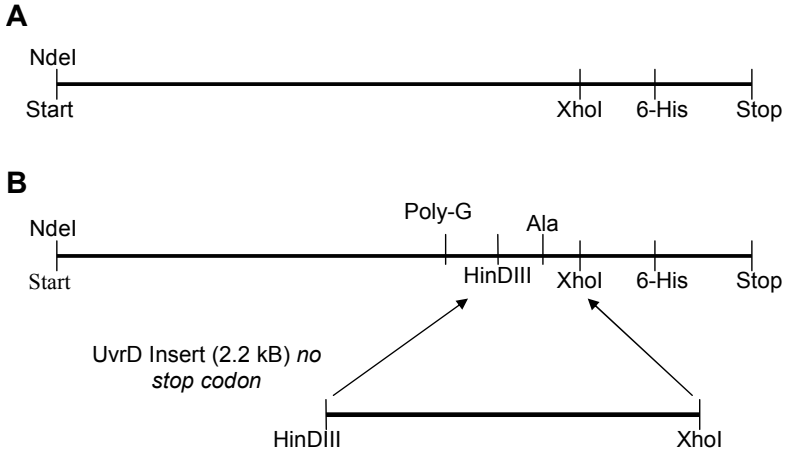

Fig. 11. Cloning strategy. A, Schematic of the Dpo4 gene in pET 22b+. B, Insertion of *E.coli* UvrD between newly-engineered HinDIII and XhoI sites.

Experimental Procedures

In order to obtain a Dpo4•UvrD fusion construct the cloning strategy in Fig.10 was devised, in which the UvrD gene is attached to the C-terminus of Dpo4 via a poly-glycine linker. While the experimental approach for this study has been designed in its entirety, the execution is lacking and a full-length fusion construct has yet to be generated. Described below is the work that has been done to date on this project.

Generation of UvrD insert. HindIII and XhoI restriction sites were added to the UvrD gene via mutagenic PCR (35 cycles: denturation, 95° C for 30 sec; annealing, 48° C for 10 min; extension, 68° C for 7 min) using the mutagenic primers UvrD-HinDIII Forward 5'–CATAAGCTTATGGACGTTTCTTACCTGCTCGACAGCC-3' and UvrD-XhoI Reverse: 5' –GTGGAGCTCCACCGACTCCAGCCG -3'. The PCR product was digested with HindIII and XhoI (New England Biolabs). The size of the insert was confirmed using a using a 0.8% agarose gel and the digested UvrD gene was purified using a QIAquick Gel Extraction Kit (Qiagen).

Insertion of the HindIII and poly-glycine linker into Dpo4 vector. Synthetic oligonucleotide primers (Table 5) were used to introduce the HindIII and poly-glycine linker into the Dpo4 gene via a site-directed mutagenesis kit using *Pfu Turbo* (Stratagene). The PCR was carried out for 18 cycles (denaturation, 95°C for 30 sec; annealing, 55°C for 1 min; extension, 68°C for 14 min) and after DpnI digestion the amplified products were transformed into the XL-10 Gold *E.coli* strain (Stratagene). Mutant plasmids were purified from transformed cells using the Wizard *Plus* SV Miniprep kit (Promega) and sequences were confirmed by OSU Plant Microbe Genomics Facility.

Table 5. DNA Primers for HindIII and poly-glycine linker in Dpo4

HindIII 3-Gly	Forward 5'-CAAGTTCTTCGATACTGGAGGTGGAAAGCTTGCACTCGAGCACCACCAC -3' Reverse 5'-GTGGTGGTGCTCGAGTGCAAGCTTTCCACCTCCAGTATCGAAGAACTTG -3'
6-Gly I	Forward 5'-CAAGTTCTTCGATACTGGAGGTGGAGGTGGAGGTGGAGGTGGAAAGCTTG -3' Reverse 5'-CAAGCTTTCCACCTCCACCTCCACCTCCACCTCCAGTATCGAAGAACTTG -3'
6-Gly II	Forward 5'-CAAGTTCTTCGATACTGGGGGAGGTGGAGGTGGAGGAGGTGGAGGTGGAGG -3' Reverse 5'-CAATTCTCCCAATACTGATTTTTGATCTATTTTCTACAGGCTCGTTATACTC -3'

Summary of Results

The full length fusion construct has yet to be generated. Progress on this project ceased upon the departure of Dr. Basavaraj Bagewadi, a postdoctoral fellow in our lab. Work will resume with the ligation of the UvrD insert to the calf-intestine alkaline phosphotase (CIAP)-

digested Dpo4 (with HindIII restriction site and poly-glycine linker) vector. The ligation will be carried out using T4 DNA ligase (New England Biolabs) overnight at 16° C. Upon generation of the full-length construct the next challenge will be purification of the fusion protein. The C-terminal His_6 tag on the Dpo4 vector will provide the first purification step, and a column which mimics DNA structure such as the Heparin Sepharose (GE Healthcare) may be used to further purify the fusion construct. Assuming that it could be purified, we would use DNA substrates of varying length to compare the processivity of wild-type Dpo4 to that of the fusion construct.

D. Purification of Human DNA Polymerase κ (hPol κ) and Mouse DNA Polymerase κ (mPol κ)

Human Y-family DNA polymerases are known to be capable of translesion synthesis [5], but the bypass of DNA lesions can be done in an error-free or an error-prone manner [30]. For that reason members of our lab have launched a project in which the mutational profile that results from the bypass process catalyzed by the human Y-family DNA polymerases η, κ, and ι on damaged DNA templates were quantitatively analyzed by a novel short oligonucleotide sequencing assay [21]. DNA polymerase κ was purified as a part of the project which aims to establish the outcome of translesion synthesis by Y-family DNA polymerases. The methods for this project have been designed in our lab and published in 2007 [21] with a model Y-family DNA polymerase, Dpo4.

Experimental Procedures

Purification of mPol κ. The N-terminal His_6-tagged mPol κ plasmid (pET 16b) was transformed into BL21(DE3) Rosetta chemical competent cells by heat shock (42° C for 45 seconds). An overnight culture of *E. coli* expression strain BL21(DE3) Rosetta carrying the mPol κ plasmid was used to inoculate Luria-Bertani medium containing 100μg/mL ampicilan, and the cells were grown at 37° C until OD_{600} = 0.6. The cultures were induced with 0.15 mM IPTG and incubated at 19° C for 10 h (OD_{600} ~1.7). Induced cells were harvested (4000 rpm,15 min) and resuspended in Buffer A (10 mM $KHPO_4$, pH 7.0, 300 mM NaCl, 10 mM $MgCl_2$, 10% glycerol, 0.1% beta-mercaptoethanol, 1 mM imidazole). EDTA-free protease inhibitor cocktail (Roche, 1 tablet) and PMSF (1 mM) were added just before the cells were lysed by passing through a French Press cell at 15,000 psi three times. The lysate was clarified by ultracentrifugation (40,000 rpm, 40 min), and the supernatant was incubated with 10 ml IMAC Fastflow6 resin (Ni^{2+} charged, GE Healthcare) and rocked slowly for 3 hours in the presence of 10 mM imidazole. The supernatant was then removed by centrifugation in a swing bucket centrifuge (2500 rpm, 2.5 min) and the resin was packed into a HR-10/10 FPLC column (GE Healthcare). The mPol κ bound to the resin was purified through a linear gradient of 35–500 mM imidazole in Buffer B (10 mM $KHPO_4$, pH 7.0, 350 mM NaCl, 5–500 mM imidazole, 10% Glycerol, 0.05% β-mercaptoethanol). Fractions containing mPolκ were dialyzed for 3 hours against dialysis Buffer C (50 mM Tris-HCl, pH 7.5 at 25° C, 50 mM NaCl, 1 mM EDTA,

10% Glycerol, 0.1% β-mercaptoethanol). The dialyzed protein solution was applied to two 5 mL HiTrap Q anion exchange columns (GE Healthcare), and eluted via a three-step gradient (100–150 mM NaCl, 150 mM NaCl, 150–1000 mM NaCl) in buffer C. Fractions containing mPol κ were dialyzed against buffer D (20 mM Tris—HCl, pH 7.5 at 25° C, 150 mM NaCl, 1 mM EDTA, 10% glycerol, 0.1% β-mercaptoethanol) for 3 h at 4° C. The dialyzed protein solution was concentrated to 4 mL using a CentriPrep YM-50 apparatus and applied to a HiLoad 26/60 Sephacryl 200 gel filtration column (GE Healthcare) and eluted in buffer D (150 mM NaCl). Fractions containing purified mPol κ were dialyzed against buffer E (25 mM HEPES, pH 7.5 at 4° C, 150 mM NaCl, 1 mM EDTA, 1 mM DTT, 50% Glycerol) and stored at -80° C. The concentration of the purified mPol κ was measured spectrophotometrically at 280 nm using the calculated extinction coefficient 31860 $M^{-1}cm^{-1}$.

Pufification of hPol κ. hPol κ was purified by the same method as mPol κ with the exception that a Heparin Sepharose column (GE Healthcare) was used in addition to the columns used for mPol κ. hPol κ was eluted from the column using a linear gradient (150–1000 mM NaCl) in buffer C. Fractions containing hPol κ were then dialyzed against buffer E and stored at -80° C The concentration of the purified mPol κ was measured spectrophotometrically at 280 nm using the calculated extinction coefficient 32,100 $M^{-1}cm^{-1}$.

Summary of Results

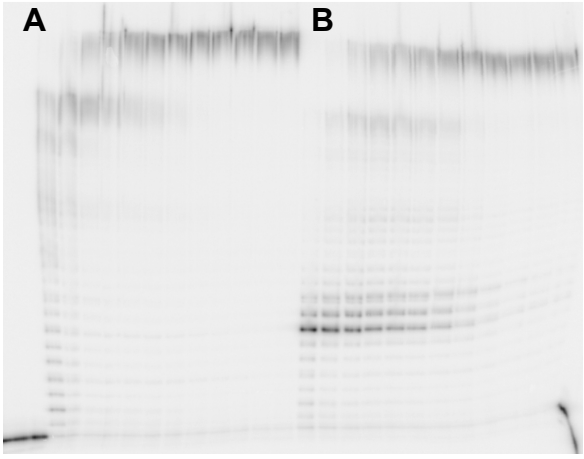

Fig. 12. Gel image showing the activity of mPolκ. A, mPolκ was given 3 h to synthesize an undamaged 14/51-mer substrate (left) to full length product. B, mPolκ efficiently bypasses an abasic site analogue (THF) in the same time frame.

By analyzing the mutational profile demonstrated by mPolκ on a DNA substrate containing an abasic site analogue (tetrahydrofuran, THF) it has been demonstrated that mPol κ preferentially incorporates adenine opposite an abasic site (28 of 44 colonies, 64%) (Pryor and Suo unpublished results), while also showing a proclivity (14%) to generate double deletions that would result in frameshift mutations. In the future similar studies will be done with other DNA lesions and the human pol κ enzyme.

E. Purification of *Sulfolobus solfataricus* DNA Polymerase B1 (SSo Pol B1) D231A, E233A, D318A Triple Substitution Mutant

The *Sulfolobus solfataricus* (Sso) genome contains two functional DNA polymerases: Dpo4 and PolB1 [31]. Because the organism survives with only two DNA polymerases, we would like to investigate the mechanism of action of these polymerases using pre-steady-state kinetics. PolB1 is considered to be the polymerase that is responsible for bulk DNA synthesis during replication, and unlike Dpo4 it stalls at the site of DNA lesions (Fig. 13). Much mechanistic insight has already been gained with Dpo4 [18], but similar analysis has not been performed with PolB1. In order to use pre-steady-state kinetics to dissect the mechanism for PolB1 it is first necessary to eliminate the robust intrinsic exonuclease activity demonstrated by PolB1 [31]. Intrinsic exonuclease activity places a severe limitation on any kinetic assay to examine the DNA polymerase activity. In order to eliminate the exonuclease activity of PolB1 site-directed mutagenesis was used to mutate to alanine the conserved aspartic acid and glutamic acid residues that bind catalytic metal ions in the exonuclease domain. Residues essential for exonuclease activity were identified using a sequence alignment of the Sso PolB1 gene with other replicative DNA polymerases [31]. Based on the sequence alignment and structural evidence [32] the residues D231, E233, D318, and D413 were identified as the residues responsible for chelating the two catalytic Mg^{2+} ions in the Sso PolB1 active site. Three of the four conserved residues were selected for mutation to alanine. The D231A, E233A, D318A PolB1 triple mutant will be tested for residual exonulease activity after the DNA substrates are available.

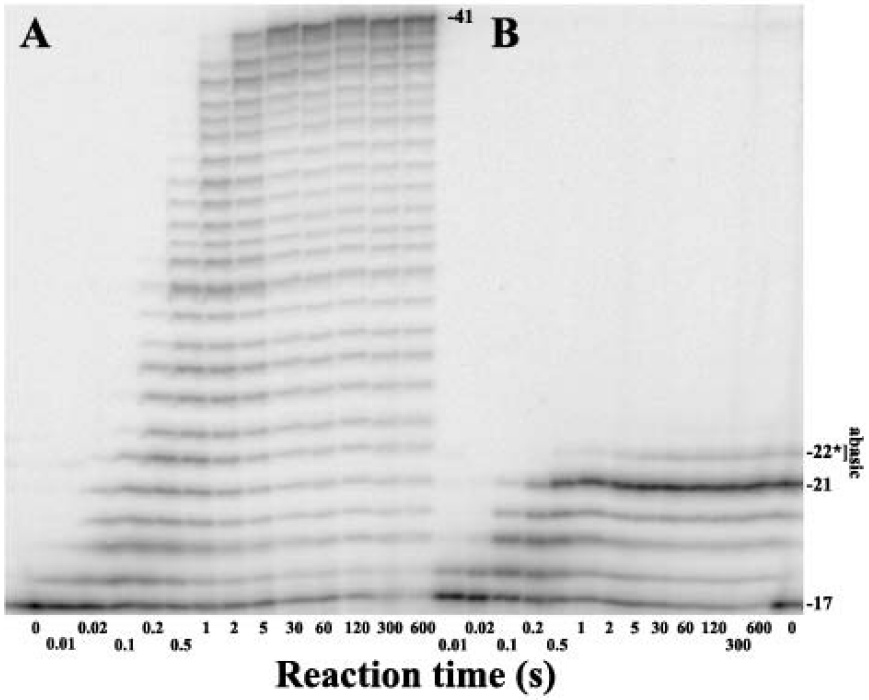

Fig. 13. SSo PolB1 stalled by an abasic site. A, undamaged 17/41-mer. B, 17/41-mer with an embedded abasic site analogue in template. Pol B1 is unable to synthesize beyond the lesion.

Experimental Procedures

Generation of the PolB1 D231A, E233A, D318A exonuclease deficient mutant. Synthetic oligonucleotide primers (Table 6) were used to introduce the single amino acid substitutions into the PolB1 gene via a site-directed mutagenesis kit using *Pfu Turbo* (Stratagene). The first two substitutions (D231A and E233A) were carried out first and the resulting plasmid was used as a template for the D318A mutation. PCR was carried out for 18 cycles (denaturation, 95°C for 30 sec; annealing, 55°C for 1 min; extension, 68°C for 14 min) and after DpnI digestion the amplified products were transformed into the XL-10 Gold *E.coli* strain (Stratagene). Mutant plasmids were purified from transformed cells using the Wizard *Plus* SV Miniprep kit (Promega) and sequences were confirmed by OSU Plant Microbe Genomics Facility.

Table 6. DNA Primers for Sso PolB1 exonuclease deficient mutant

D231A E233A	Forward 5'-AAAAGGGTTGCGATA**GCC**ATT**GCG**GTATATACACCAGTTAAG -3' Reverse 5'-AACTGGTGTATATAC**CGC**AAT**GGC**TATCGCAACCCTTTTTATTTTAG -3'
D318A	Forward 5'-CAATGGAGACGATTTT**GCT**TTACCTTACATTTAC -3' Reverse 5'-GTAAATGTAAGGTAA**AGC**AAAATCGTCTCCATTG -3'

Purification of Sso Pol B1 D231A, E233A, D318A. The N-terminal His_6-tagged PolB1 D231A, E233A, D318A plasmid (pET34b) was transformed into BL21(DE3) Rosetta chemical competent cells by heat shock (42° C for 45 seconds). An overnight culture of *E. coli* expression strain BL21(DE3) Rosetta carrying the polB1 plasmid was used to inoculate Luria-Bertani medium containing 50 µg/mL kanamycin and 25 µg/mL chloramphenicol, and the cells were grown at 37° C until OD_{600} = 0.6. The cultures were induced with 0.15 mM IPTG and incubated at 25° C for 7.5 h (OD_{600} ~1.7). Induced cells were harvested (4000 rpm,15 min) and resuspended in Buffer A (10 mM $KHPO_4$, pH 7.0, 50 mM NaCl, 10 mM $MgCl_2$, 10% glycerol, 0.1% beta-mercaptoethanol, 1 mM imidazole). EDTA-free protease inhibitor cocktail (Roche, 1 tablet) and PMSF (1 mM) was added just before the cells were lysed by passing through a French Press cell at 15,000 psi three times, and the lysate was clarified by ultracentrifugation (40,000 rpm, 40 min). Cleared lysate was subjected to heat denaturation at 74° C for 14 min to precipitate thermolabile *E. coli* proteins which were then removed by ultracentrifugation (40,000 rpm, 40 min). The supernatant was incubated with 8 ml IMAC Fastflow6 resin (Ni^{2+} charged, GE Healthcare) and rocked slowly for 3 hours in the presence of 10 mM imidazole. The supernatant was then removed by centrifugation in a swing bucket

centrifuge (2500 rpm, 2.5 min) and the resin was packed into a HR-10/10 FPLC column (GE Healthcare). The PolB1 bound to the resin was purified through a linear gradient of 35–500 mM imidazole in Buffer B (10 mM $KHPO_4$, pH 7.0, 350 mM NaCl, 5–500 mM Imidazole, 10% Glycerol, 0.05% β-mercaptoethanol). Fractions containing PolB1 were dialyzed for 3 hours against dialysis Buffer C (50 mM Tris-HCl, pH 7.5 at 25° C, 50 mM NaCl, 1 mM EDTA, 10% Glycerol, 0.1% β-mercaptoethanol). The dialyzed protein solution was passed through two 5 mL HiTrap Q anion exchange columns (GE Healthcare). The loading elute was applied to two 5 mL HiTrap SP cation exchange columns (GE Healthcare) and eluted using a gradient of 100—1000 mM NaCl in buffer C. The fractions containing PolB1 were dialyzed against buffer D (25 mM HEPES, pH 7.0 at 4° C, 150 mM NaCl, 1 mM EDTA, 1 mM DTT, 50% Glycerol) and stored at -80° C. The concentrations of the purified PolB1 mutants were measured spectrophotometrically at 280 nm using the calculated extinction coefficient 124,785 $M^{-1}cm^{-1}$.

Summary of Results

The PolB1 D231A, E233A, D318A triple substitution mutant has been purified to apparent homogeneity (Fig. 14), but no further studies have been done to date. The enzyme will be tested for exonuclease activity by incubating the enzyme with a 5' ^{32}P-labeled DNA substrate in the presence of Mg^{2+}. A marked degradation pattern will be readily visible if the enzyme still possesses exonuclease activity.

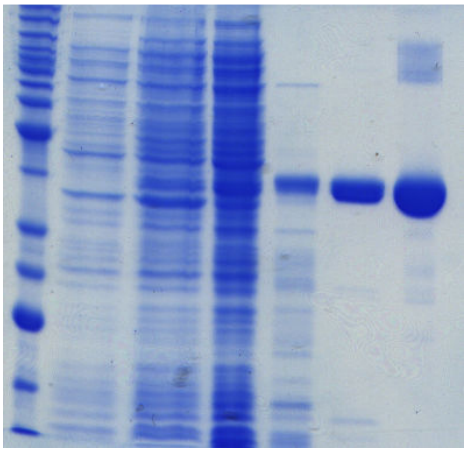

Fig. 14. SDS PAGE gel showing the purification of PolB1

References

1. Zhong, D., *Ultrafast catalytic processes in enzymes.* Curr Opin Chem Biol, 2007. **11**(2): p. 174-81.
2. Garcia-Diaz, M.*, et al.*, *A closed conformation for the Pol lambda catalytic cycle.* Nat Struct Mol Biol, 2005. **12**(1): p. 97-8.
3. Ling, H.*, et al.*, *Crystal structure of a Y-family DNA polymerase in action: a mechanism for error-prone and lesion-bypass replication.* Cell, 2001. **107**(1): p. 91-102.
4. Jackson, S.P., *Detection, Repair and Signalling of DNA Double-Strand Breaks.* Biochem. Soc. Trans., 1999. **27**: p. 1-13.
5. Rattray, A.J. and J.N. Strathern, *Error-prone DNA polymerases: when making a mistake is the only way to get ahead.* Annu Rev Genet, 2003. **37**: p. 31-66.
6. Aoufouchi, S.*, et al.*, *Two novel human and mouse DNA polymerases of the polX family.* Nucleic Acids Res, 2000. **28**(18): p. 3684-93.
7. Garcia-Diaz, M.*, et al.*, *DNA polymerase lambda (Pol lambda), a novel eukaryotic DNA polymerase with a potential role in meiosis.* J Mol Biol, 2000. **301**(4): p. 851-67.
8. Lindahl, T. and R.D. Wood, *Quality control by DNA repair.* Science, 1999. **286**(5446): p. 1897-905.
9. Beard, W.A. and S.H. Wilson, *Structural design of a eukaryotic DNA repair polymerase: DNA polymerase beta.* Mutat Res, 2000. **460**(3-4): p. 231-44.
10. Braithwaite, E.K.*, et al.*, *DNA polymerase lambda mediates a back-up base excision repair activity in extracts of mouse embryonic fibroblasts.* J Biol Chem, 2005. **280**(18): p. 18469-75.
11. Fiala, K.A., W. Abdel-Gawad, and Z. Suo, *Pre-steady-state kinetic studies of the fidelity and mechanism of polymerization catalyzed by truncated human DNA polymerase lambda.* Biochemistry, 2004. **43**(21): p. 6751-62.
12. Bertocci, B.*, et al.*, *Nonoverlapping functions of DNA polymerases mu, lambda, and terminal deoxynucleotidyltransferase during immunoglobulin V(D)J recombination in vivo.* Immunity, 2006. **25**(1): p. 31-41.
13. Lee, J.W.*, et al.*, *Implication of DNA polymerase lambda in alignment-based gap filling for nonhomologous DNA end joining in human nuclear extracts.* J Biol Chem, 2004. **279**(1): p. 805-11.
14. Ahn, J., B.G. Werneburg, and M.D. Tsai, *DNA polymerase beta: structure-fidelity relationship from Pre-steady-state kinetic analyses of all possible correct and incorrect base pairs for wild type and R283A mutant.* Biochemistry, 1997. **36**(5): p. 1100-7.
15. Sawaya, M.R.*, et al.*, *Crystal structures of human DNA polymerase beta complexed with gapped and nicked DNA: evidence for an induced fit mechanism.* Biochemistry, 1997. **36**(37): p. 11205-15.
16. Jackson, S.P., *Colworth Medal lecture. Detection, repair and signalling of DNA double-strand breaks.* Biochem Soc Trans, 1999. **27**(2): p. 1-13.
17. Goodman, M.F., *Error-prone repair DNA polymerases in prokaryotes and eukaryotes.* Annu Rev Biochem, 2002. **71**: p. 17-50.
18. Fiala, K.A. and Z. Suo, *Pre-steady-state kinetic studies of the fidelity of Sulfolobus solfataricus P2 DNA polymerase IV.* Biochemistry, 2004. **43**(7): p. 2106-15.
19. Fiala, K.A.*, et al.*, *Mechanism of template-independent nucleotide incorporation catalyzed by a template-dependent DNA polymerase.* J Mol Biol, 2007. **365**(3): p. 590-602.

20. Fiala, K.A., C.D. Hypes, and Z. Suo, *Mechanism of abasic lesion bypass catalyzed by a Y-family DNA polymerase.* J Biol Chem, 2007. **282**(11): p. 8188-98.
21. Fiala, K.A. and Z. Suo, *Sloppy bypass of an abasic lesion catalyzed by a Y-family DNA polymerase.* J Biol Chem, 2007. **282**(11): p. 8199-206.
22. Boudsocq, F.*, et al.*, *Investigating the role of the little finger domain of Y-family DNA polymerases in low fidelity synthesis and translesion replication.* J Biol Chem, 2004. **279**(31): p. 32932-40.
23. Stites, W.E. and J. Pranata, *Empirical evaluation of the influence of side chains on the conformational entropy of the polypeptide backbone.* Proteins, 1995. **22**(2): p. 132-40.
24. Golinelli, M.P. and S.H. Hughes, *Nontemplated base addition by HIV-1 RT can induce nonspecific strand transfer in vitro.* Virology, 2002. **294**(1): p. 122-34.
25. Patel, P.H. and B.D. Preston, *Marked infidelity of human immunodeficiency virus type 1 reverse transcriptase at RNA and DNA template ends.* Proc Natl Acad Sci U S A, 1994. **91**(2): p. 549-53.
26. Golinelli, M.P. and S.H. Hughes, *Nontemplated nucleotide addition by HIV-1 reverse transcriptase.* Biochemistry, 2002. **41**(18): p. 5894-906.
27. Bjornson, K.P.*, et al.*, *Kinetic mechanism for the sequential binding of two single-stranded oligodeoxynucleotides to the Escherichia coli Rep helicase dimer.* Biochemistry, 1998. **37**(3): p. 891-9.
28. Runyon, G.T., I. Wong, and T.M. Lohman, *Overexpression, purification, DNA binding, and dimerization of the Escherichia coli uvrD gene product (helicase II).* Biochemistry, 1993. **32**(2): p. 602-12.
29. Hickson, I.D.*, et al.*, *The E. coli uvrD gene product is DNA helicase II.* Mol Gen Genet, 1983. **190**(2): p. 265-70.
30. Pages, V. and R.P. Fuchs, *How DNA lesions are turned into mutations within cells?* Oncogene, 2002. **21**(58): p. 8957-66.
31. Pisani, F.M., C. De Martino, and M. Rossi, *A DNA polymerase from the archaeon Sulfolobus solfataricus shows sequence similarity to family B DNA polymerases.* Nucleic Acids Res, 1992. **20**(11): p. 2711-6.
32. Savino, C.*, et al.*, *Insights into DNA replication: the crystal structure of DNA polymerase B1 from the archaeon Sulfolobus solfataricus.* Structure, 2004. **12**(11): p. 2001-8.